Phys. Status Solidi A **214,** No. 8, 1700135 (2017) / **DOI** 10.1002/pssa.201700135

physica status solidi a
www.pss-a.com
applications and materials science

Surfactant free template assisted electrodeposited n-type nano-cubic Cu_2O thin films for nonenzymatic glucose sensing

J. L. K. Jayasingha[1], M. N. Kaumal[2], K. M. D. C. Jayathilaka[3], M. S. Gunewardene[1], D. P. Dissanayake[2], and J. K. D. S. Jayanetti[*,1]

[1] Department of Physics, University of Colombo, Colombo 03, Sri Lanka
[2] Department of Chemistry, University of Colombo, Colombo 03, Sri Lanka
[3] Department of Physics, University of Kelaniya, Kelaniya, Sri Lanka

Received 8 March 2017, revised 5 April 2017, accepted 19 April 2017
Published online 5 May 2017

Keywords amperometric measurements, Cu_2O nanocubes, electrodeposition, glucose sensing

[*] Corresponding author: e-mail sumedhajayanetti@gmail.com, Phone/Fax: +94 112584777

Amperometric sensing measurements of glucose were performed using n-Cu_2O nano-cubic films fabricated on Ti using a surfactant free template aided electrodeposition method. The electrochemical performance of these films in the presence of aqueous glucose was characterized by cyclic voltammetry and chronoamperometry. Amperometric sensing measurements of glucose for the nano-cubic Cu_2O/Ti electrode were significantly better than the microcrystalline counterpart prepared under similar electrodeposition conditions without the aid of a template. Measurements yielded a sensitivity of $28.4 \pm 0.2\,\mu A\,mM^{-1}\,cm^{-2}$ at an applied potential of +0.6 V with a lower detection limit of 15.6 μM and a linear range of detection from 17 to 11,650 μM. The linear range is one of the best ever reported, for a copper oxide-based amperometric glucose sensing electrode. Films were characterized using XRD and SEM.

1 Introduction Cu_2O is a well-known oxide semiconductor with a direct band gap of ~2.0 eV and is considered an earth abundant green material with a great potential to be used in many applications such as photovoltaics [1–3], gas sensing [4, 5], electro-catalysis [6, 7], and photo-catalysis [8, 9]. As a semiconductor, the carrier concentration of Cu_2O is relatively low ($\sim 10^{14}$–$10^{15}\,cm^{-3}$) [4]. Therefore, from a sensing material perspective, to improving the charge transport characteristics and adsorption capacity of Cu_2O thin films and modulating their morphology at a nanoscale is considered important because it leads to reduced recombination of carriers [1]. Also, the high surface to volume ratio that can be achieved at a nanoscale assists the charge carrier generation through the associated physical/chemical sensing process. Yet, the increased number of grain boundaries at a nanoscale may give rise to more defect sites and thus leading to limitations in the sensor performance. Therefore, to maximize the sensor performance, careful attention is required for the optimization of surface morphology in terms of both size and shape. Due to the presence of Cu vacancies in the crystal lattice, Cu_2O has been generally known as a p-type semiconductor [5, 9, 10]. However, it has now been established that by employing electrochemical deposition technique, the conductivity of Cu_2O can be easily controlled to grow both p-type and n-type thin films [1, 5, 11], compared to other fabrication techniques such as facile hydrothermal process [2], fixure-reduction method [12], and wet chemistry synthesis [13]. Additionally, the scalability and the ability to grow films with different surface morphologies are advantages of the electrochemical deposition technique [11, 14, 15]. It is known that the resultant surface morphology of the thin films is highly sensitive to a variation of the electrolytic bath conditions such as pH, temperature and concentration of the constituent ions in the bath, the applied electrode potential and the deposition current density across the electrode surface [11]. Glucose sensing is of utmost importance from a biomedical point of view, as glucose has an impact on the human health and safety. A reliable and fast determination of

glucose is important in areas such as clinical diagnostics, biotechnology, and food chemistry [16–20]. In recent times, many efforts have been made in the use of non-enzymatic electrochemical sensors for the detection of glucose using amperometric measurements, where both CuO and Cu_2O-based electrodes have been employed. CuO nano-cube–graphene nanocomposite modified glassy carbon electrodes (CuO–G–GCE) [20], CuO nanoparticles modified multi-walled carbon nanotube (MWCNTs) array electrodes [18], CuO grown on Ti substrates [21], CuO nanosphere added glassy carbon (GC) electrodes [22], CuO graphene nano-composite electrodes [17], and modified graphite substrates by the synthesis of CuO flowers and nanorods [23] are some of the examples available in literature for the use of CuO-based electrodes for glucose detection. An equally impressive list of research articles is available on the use of Cu_2O-based electrodes for glucose detection. Sensitivities in varying ranges with good detection limits have been achieved in these studies using sensor electrodes such as Cu_2O/MWCNT nanocomposites [12], Cu_2O/Cu [24], Cu/Cu_2O hollow micro-spheres [25], Cu_2O and Au/Cu_2O particles [6], graphene-wrapped Cu_2O nano-cubes [26], Cu_2O nano-cubes [27], and carbon quantum dots/octahedral Cu_2O nano composites [28] fabricated using chemical methods.

The objective of this study is to show the enhancement in sensing performances for amperometric measurements in the presence of glucose when surface morphology is changed from micro to nanoscale by fabricating n-type Cu_2O thin films with cubic nanostructures. Fabrication of the films was done by electrochemical deposition using a template-assisted surfactant free fabrication method [1]. Despite the simplicity of the fabrication method that involves only morphological manipulation of a single material (Cu_2O), the linear range results obtained for glucose sensing can be rated as very high compared to the values reported in literature. n-type Cu_2O electrodes with cubic nanostructures also show significantly better sensitivity and lower detection limits compared to their microcrystalline counterparts.

2 Experimental The electrochemical deposition set up consisted of a saturated calomel electrode (SCE) as the reference electrode, and a platinum plate as the counter electrode, respectively. A potentiostatic deposition of Cu_2O was carried out using Hokuto-Denko-Potentiostat/Galvanostat-HA301 at an applied potential of -200 mV versus SCE. Films were deposited on both Ti substrates and on n-type Cu_2O templates fabricated on Ti plates. The p-type conductivity of as deposited nano-cubic templates were converted into n-type conductivity by annealing at 200 °C under the atmospheric air in a tube furnace (ISUZU Micro Computer Controller). The deposition bath contained 0.1 M sodium acetate (Sigma–Aldrich, purity $\geq$99.0%), and 0.01 M cupric acetate (Sigma–Aldrich, purity $\geq$99.0%), while the pH of the bath was controlled using aqueous 2.0 M NaOH (Sigma–Aldrich, purity $\geq$98.0%) solution. A more detailed procedure of the fabrication of nano-cubic n-type Cu_2O film structures has been reported elsewhere [4]. The temperature of the bath was maintained at the desired value and the bath was stirred constantly during electrodeposition. The films and conditions used to generate them are given in Table 1.

Conductivity of the resulting films was measured using photocurrent spectral response measurements by exposing a small area ($\sim$4 mm^2) of the films in a three electrode electrochemical cell containing a 0.1 M sodium acetate solution. The counter electrode and the reference electrode were a Pt sheet and the SCE, respectively. The photocurrent spectral response measurements were obtained using a phase sensitive detection method by chopping a monochromatic light beam at a chopping frequency of 60 Hz. The experimental setup consisted of a lock-in-amplifier

Table 1 Conditions used to prepare Cu_2O films.

Cu_2O films	label	substrate	pH	temp. (°C)	deposition time (min)	treatments	conductivity
as deposited template	–	Ti plate	7.6	60	30	not annealed	p-type
template (annealed)	–	Ti plate	7.6	60	30	after the deposition, annealed for 5 min at 200 °C	n-type
Cu_2O film deposited on annealed template	T_{20}	template	6.0	60	20	not annealed	n-type
Cu_2O film deposited on annealed template	T_{30}	template	6.0	60	30	not annealed	n-type
Cu_2O film deposited on annealed template	T_{40}	template	6.0	60	40	not annealed	n-type
Cu_2O film deposited on annealed template	T_{50}	template	6.0	60	50	not annealed	n-type
Cu_2O film deposited on annealed template	T_{60}	template	6.0	60	60	not annealed	n-type
Cu_2O film deposited on bare Ti substrate	S_{60}	Ti plate	6.0	60	60	not annealed	n-type

(Stanford Research-SR 830 DSP), a potentiostat (Hokuto Denko HAB-151), a chopper (Stanford-SR 540) and a monochromator (Sciencetech-9010). The surface morphological variations and the structure of the deposited Cu_2O films were monitored using scanning electron microscopy (Zeiss Evols15) and X-ray diffractometry (Rigaku/Ultima-iv) with Cu-K_α ($\lambda = 1.5418$ Å) as the source of X-rays, respectively.

Electrochemical measurements of glucose sensing were accomplished using a Ziew SP5 electrochemical workstation. A conventional three-electrode system was used with Ag/AgCl as the reference electrode, a platinum sheet as the counter electrode, and the above-described Cu_2O films as the working electrode. An analytical grade D-Glucose (Sigma–Aldrich) was used and all the solutions were freshly prepared with deionized water. The amperometric measurements were carried out by adding the relevant amount of glucose of 0.05, 0.1, and 1 mM into a 0.1 M NaOH electrolyte under continuous stirring conditions at room temperature. The applied potential was +0.6 V. For each measurement, the electrolyte was deaerated with nitrogen gas for 10 min. The possible interference effects from chemicals such as ascorbic acid (AA), citric acid (CA), uric acid (UA), and NaCl were tested by adding 0.1 mM AA, 0.1 mM CA, 0.1 mM UA, and 0.1 mM NaCl. The cyclic voltammograms were obtained in 0.1 M NaOH electrolyte at room temperature (25 °C).

3 Results and discussion Electrodeposited Cu_2O thin films, where the type of main transport carriers (electrons or holes) can be controlled, were produced using a surfactant free template-assisted method on Ti having nano-cubic morphology. These n-Cu_2O/Ti electrodes were used for amperometric measurements of glucose and were compared with microcrystalline counterpart, in order to highlight the role played by film thickness and geometric shape and thus, the lateral coverage area involved on the glucose sensing. Particularly, the deposition bath conditions were varied to control the morphological properties of the thin films. Figure 1 shows the SEM image of a nano-cubic p-type Cu_2O thin film template deposited on Ti substrate in an acetate bath containing 0.1 M sodium acetate and 0.01 M cupric acetate at pH of 7.6 for 30 min at 60 °C. It was found that the morphology of the electrodeposited films was strongly dependent on the pH of the electrolyte.

Cu_2O nano-cubes having dimensions ranging from approximately 150–300 nm are clearly seen in Fig. 1.

Previous work by Won and Stanciu [6] reports larger cubic crystals in the range of 800 nm–1 μm obtained using chemical bath deposition. The thickness of the films was calculated using Faraday's equation mentioned elsewhere [5, 29].

Figure 2(a)–(e) shows the SEM images of n-type Cu_2O films fabricated using Cu_2O nano-cubic templates and (f) corresponds to the n-Cu_2O fabricated on a bare Ti substrate. With the increase in deposition time, the changes

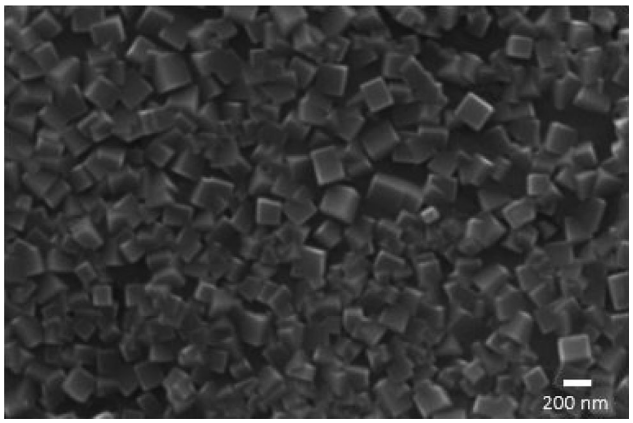

Figure 1 Scanning electron microscopic image of Cu_2O nano-cubes on Ti substrate fabricated in an acetate bath containing 0.1 M sodium acetate and 0.01 M cupric acetate of pH 7.6 at 60 °C for 30 min (template). The thickness of the nano-cubic thin film is ~500 nm.

in morphology are well apparent in template-assisted electrodeposited Cu_2O films. Figure 2(a) and (b) both show an agglomeration of a large number of nano-cubic crystals where the size distribution of nanocubes are smaller in the film shown in Fig. 2(b). However, in Fig. 2(c) the morphology has changed to structures that have deviated from nano-cubic crystallinity which eventually leads to arbitrary-shaped microcrystalline structures as shown in Fig. 2(d) and (e). Therefore, it can be seen that the fabrication of cubic nanostructures on templates is restricted to a certain limit of deposition time and thus, the film thickness. Consequently, a gradual decrease in the film surface area is observed beyond a deposition time of 30 min.

Figure 3 shows the X-ray diffraction spectra obtained for the as-deposited nano-cubic template, the nano-cubic template after annealing at 200 °C for 5 min, the electrodeposited Cu_2O thin films deposited at pH 6.0 on annealed nano-cubic template for 20 min (T_{20}), 30 min (T_{30}), 40 min (T_{40}), 50 min (T_{50}), 60 min (T_{60}), and deposited on a bare Ti substrate for 60 min (S_{60}), respectively. X-ray diffraction spectra were acquired for all samples for a fixed time at a scan rate of $2^\circ\ min^{-1}$ and were in agreement with the standard data for Cu_2O (JCPDS: 01-2076). It can be clearly seen that even though the electrodeposition conditions have led to changes in the film morphology, the film stoichiometry has remained intact. Further, the gradual increase in the intensities of the Cu_2O diffraction peaks is a reflection of the increase of film thickness as a function of the deposition time. It is evident from these results that both the size and shape can be controlled by fine tuning the fabrication method without disturbing the stoichiometry of the films.

Figure 4 shows that the photocurrent spectral response patterns corresponding to as deposited nano-cubic template, template after annealing at 200 °C, microcrystalline thin film (S_{60}), nano-cubic thin film (T_{30}), and the film (T_{40})

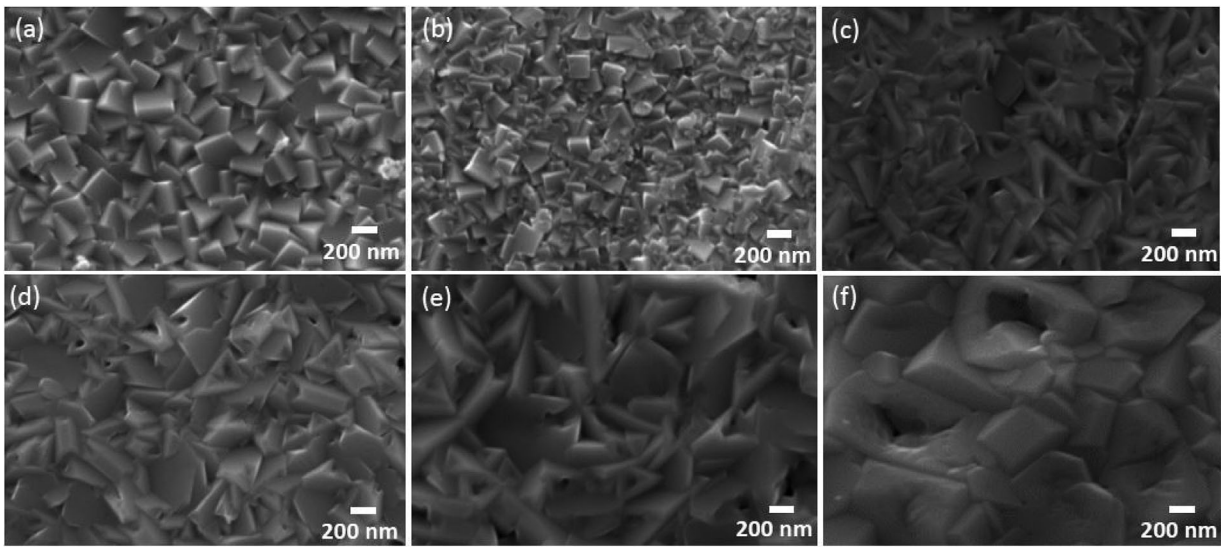

Figure 2 SEM images of electrodeposited Cu_2O thin films deposited at pH 6.0 on nano-cubic template annealed at 200 °C for 5 min for (a) 20 min (T_{20}), (b) 30 min (T_{30}), (c) 40 min (T_{40}), (d) 50 min (T_{50}), (e) 60 min (T_{60}), and (f) deposited on bare Ti substrate for 60 min (S_{60}). The thickness of the films from (a) to (f) are 1.1, 1.3, 1.6, 1.8, 2.2, and 2 μm, respectively.

that shows the onset of deviation in morphology from nano-cubic crystallinity. The spectral response plot, corresponding to nano-cubic Cu_2O template deposited at a pH of 7.6, has given a negative photocurrent indicating its p-type conductivity, while plots corresponding to all other Cu_2O thin films, T_{30}, T_{40}, and S_{60}, show a positive photocurrent, indicating that these films are of n-type conductivity.

Observations made on the morphological and thickness changes of films during the SEM and XRD measurements were also reminiscent from the spectral response measurements shown in Fig. 4. The intensities of the spectral response peaks indicate that the light harvesting properties were better for films deposited using the template (T_{30} and T_{40}), with the thicker T_{40} film showing a higher photo response compared to the nano-cubic T_{30} film that has the largest surface area. On the other hand, the thickest microcrystalline film S_{60} shows a weaker photo response compared to both T_{30} and T_{40} films, indicating that both the thickness and film morphology (larger surface area) contribute to better photo response properties.

The electrochemical properties of the electrodes are often investigated by cyclic voltammograms (CVs). As shown in Fig. 5(a) and (b), in the range of scan rates 25–200 mV s^{-1} in a 0.1 M NaOH solution in the presence of 1 mM glucose, the oxidation peak current increased linearly with increasing scan rate, implying that the electrochemical oxidation of glucose on Cu_2O/Ti is a surface-controlled process [18]. It can be seen that, upon addition of glucose to the electrolyte (1.0 mM), the oxidation process occurs in between +0.1 and +0.6 V. Compared to Cu_2O electrodes fabricated on glassy carbon [28], the Cu_2O/Ti electrodes reported in this study exhibited a broader electrocatalytic range. Among the electrodes, T_{30} with a nano-cubic crystalline structure with a thickness of ~1.2 μm shows the highest catalytic activity compared to S_{60} with thicknesses of ~2 μm. The high electrocatalytic activity of T_{30} can be attributed to the presence of a large effective

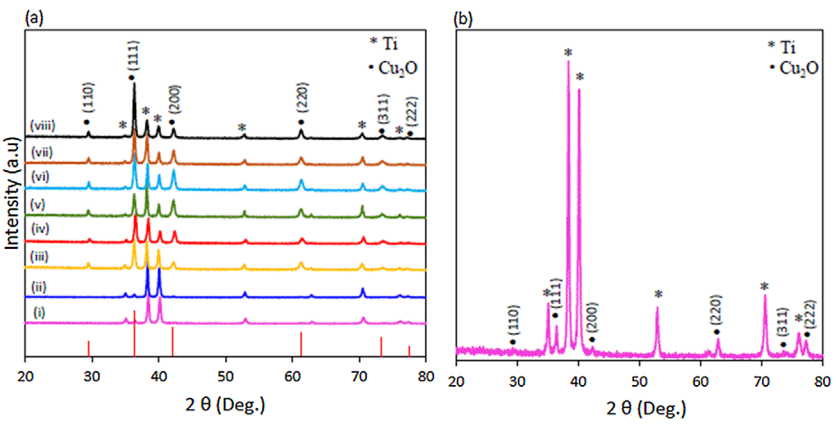

Figure 3 (a) X-ray diffraction images of (i) as-deposited nano-cubic template, (ii) nano-cubic template after annealing at 200 °C for 5 min, electrodeposited Cu_2O thin films deposited at pH 6.0 on annealed nano-cubic template for (iii) 20 min (T_{20}), (iv) 30 min (T_{30}), (v) 40 min (T_{40}), (vi) 50 min (T_{50}), (vii) 60 min (T_{60}), and (viii) deposited on bare Ti substrate for 60 min (S_{60}) in comparison with the standard data for Cu_2O (JCPDS: 01-2076). (b) An enlarged view of the X-ray diffraction pattern of as-deposited nano-cubic template.

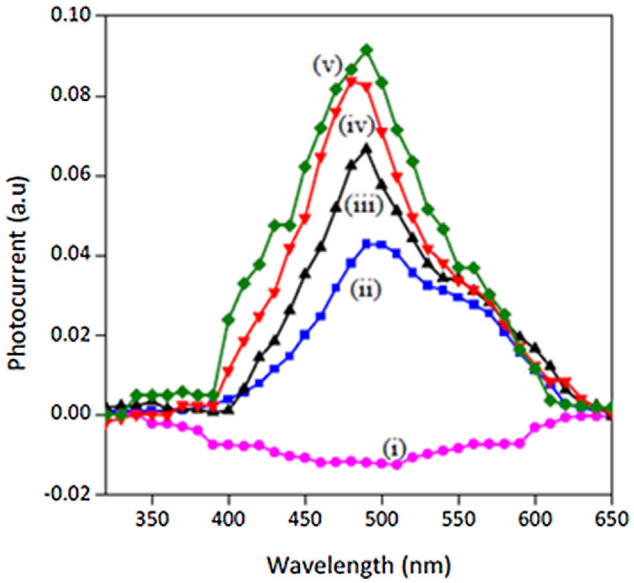

Figure 4 Photocurrent spectral response of (i) as-deposited nano-cubic Cu_2O template, (ii) nano-cubic Cu_2O template after annealing at 200 °C, (iii) microcrystalline Cu_2O thin film (S_{60}), (iv) thicker nano-cubic Cu_2O film deposited on a template for 30 min (T_{30}) in an acetate bath of pH 6.0, and (v) a thicker Cu_2O film deposited on a template for 40 min (T_{40}) in an acetate bath of pH 6.0.

surface area with Cu_2O cubic crystals. The influence of the scan rate on the current response for the anodic and cathodic processes is shown in Fig. 5. It can be seen that the anodic (I_{pa}) and cathodic (I_{pc}) peak currents of glucose oxidation are proportional to the scan rate and a linear relationship between the square root of the scan rate ($V^{1/2}$) and peak current (I) can be obtained [30]. The obtained relationship of T_{30} film is given by the equations as follows:

$$I_{pa}(\mu A) = -2.1237 + 0.9454V^{1/2}(V),\ R^2 = 0.993$$
$$I_{pc}(\mu A) = 3.7965 - 0.8749V^{1/2}(V),\ R^2 = 0.997$$

The T_{30} electrode showed the highest oxidation and reduction peak currents indicating that glucose oxidation is more efficient on this electrode. The similar observation has been made by Li et al. [28]. It can also be seen that there is a substantially negative shift in peak potential with the increase in scan rate. Wang et al. [24] have made similar observations for glucose oxidation with Cu_2O/Cu during different scan rates of 0.02–0.20 V s^{-1}. T_{30} electrode showed a better linear relationship between peak currents and the square root of scan rate compared to those in S_{60} electrode.

The oxidation peak corresponds to the conversion of Cu(II) to Cu(III), where a larger oxidation peak could be observed for nano-cubic structure. This suggests that the electrocatalytic ability of the nano-cubic structures is higher than that of microstructured Cu_2O electrodes. The mechanism of an electro-oxidation of glucose has been already reported elsewhere [28, 31].

Figure 6 shows the amperometric response of nano-cubic Cu_2O electrode (T_{30}) to glucose in 0.1 M NaOH with a successive addition of 0.1 mM gluocose after every 50 s. It also confirms that the highest electrocatalytic activity occurs around +0.5 V, and this is in agreement with cyclic voltametry experiments. In addition, a relatively high electrocatalytic activity can be seen with a better linear range at +0.6 V. Therefore, +0.6 V was considered as the optimal applied potential for amperometric measurements. It is also worth noting that microcrystalline (S_{60}) n-Cu_2O thin film electrodes had to be subjected to an applied potential of +0.6 V to yield an optimal linear range. Figure 7 shows the chronoamperometric response of Cu_2O/Ti electrodes.

It is responsible for the average response values of five consecutive data sets. Data were obtained by a successive addition of glucose in a 0.1 M NaOH solution at a working potential of +0.6 V. The response of the electrodes to glucose is rapid and steady state was reached within 6 s. Nano-cubic Cu_2O electrode (T_{30}) showed the highest response to glucose. It can be seen that the response varies linearly with glucose concentration. Also, a similar sensor performance can be obtained after more than 20 cycles. The corresponding fitted line and the response equations using a linear regression for the electrodes are shown in Fig. 7(b),

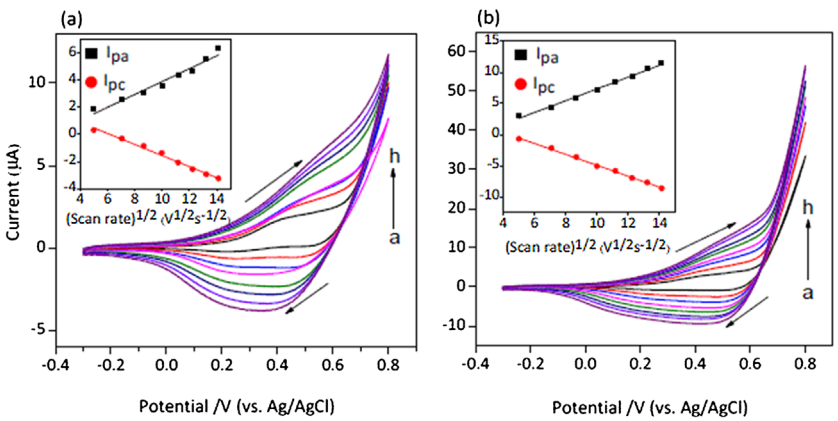

Figure 5 Cyclic voltammograms of Cu_2O/Ti electrode in a 0.10 M NaOH in the presence of 1 mM glucose at different potential scan rates of (a → h) 25, 50, 75, 100, 125, 150, 175, 200 mV s^{-1}, respectively. The electrodeposited Cu_2O thin films deposited at 60 °C and pH 6.0 (a) S_{60} (b) T_{30}. Inset: the cathodic and anodic peak currents of S_{60} and T_{30} electrodes as a function of square root of scan rate.

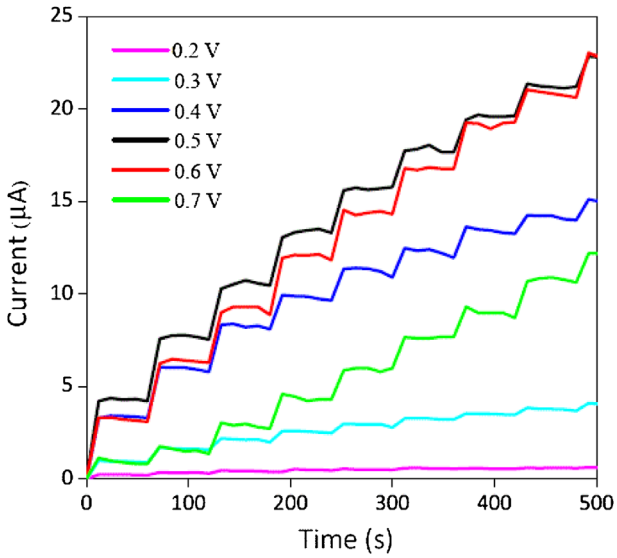

Figure 6 Amperometric responses of T_{30} electrode at different potentials in the range from +0.2 to +0.7 V in a 0.1 M NaOH electrolyte in the presence of 0.1 mM glucose.

with the slope of the fitted line providing the sensitivity for a given electrode.

The electrode T_{30} showed the highest sensitivity $(28.4 \pm 0.2)\,\mu A\,mM^{-1}\,cm^{-2}$, while the S_{60} electrode showed a sensitivity of $(16.3 \pm 0.2)\,\mu A\,mM^{-1}\,cm^{-2}$. The high sensitivity for the T_{30} electrode compared with the S_{60} electrode can be considered as a direct effect of high surface area introduced into the T_{30} electrode by the nano-cubic structures. Surface structure dependence of electrochemical performance has been previously observed by Wanga et al. [23]. The linear range of glucose sensing for electrodes T_{30} and S_{60} are 17–11,650 μM and 30–9650 μM, respectively. The measured glucose detection limits (LODs) for electrodes T_{30} and S_{60} using $3s/\sigma$, where s and σ are the standard deviation of the background current and the slope of the calibration curve, were 15.6 and 28.1 μM, respectively. A summary of a Cu_2O-based electrode response for glucose sensing reported in literature is given in Table 2 and confirms that the nano-cubic n-Cu_2O/Ti electrodes reported in this study show a greater linear range.

Experiments were conducted in order to check the interference with glucose detection by the electrodes from electroactive compounds such as AA, UA, CA, and NaCl, which commonly exist in human blood.

Figure 8 shows the response of electrodes of S_{60} and T_{30} to glucose in the presence of the above substances. These results show that Cu_2O/Ti electrodes exhibit good selectivity to glucose. Figure 8 also shows that the addition of NaCl does not alter the glucose sensing of the electrodes. It can be observed that other species such as AA, UA, and CA did not significantly interfere with glucose detection. Furthermore, the stability of the sensor was evaluated weekly for a period of 3 weeks. The current response of the Cu_2O/Ti electrode decreased to approximately 80% of its original value during this period.

4 Conclusions n-Cu_2O films with a nano-cubic surface morphology were grown on thin nano-cubic templates, fabricated on Ti plates using a surfactant free template-assisted electrodeposition method. Films maintained their nano-cubic surface morphology only up to a certain limit of film thickness beyond which the film morphology changed to arbitrary-shaped microcrystalline structures. The films with a nano-cubic surface morphology were used as electrodes to construct non-enzymatic electrochemical sensors for the detection of glucose. The electrode (T_{30}) with a nano-cubic surface morphology displayed the highest electrocatalytic activity toward the oxidation of glucose. Amperometric sensing measurements of glucose for this nano-cubic Cu_2O/Ti electrode yielded a sensitivity of $28.4 \pm 0.2\,\mu A\,mM^{-1}\,cm^{-2}$ at an applied potential of +0.6 V with a lower detection limit of 15.6 μM and a linear range of detection from 17 to 11,650 μM. In comparison, the sensitivity, the linear range, and the detection limit for the electrode (S_{60}) with a microcrystalline surface morphology were $16.3 \pm 0.2\,\mu A\,mM^{-1}\,cm^{-2}$, 30–9650 μM, 28.1 μM, respectively. Both types of electrodes which were stable for long periods did not produce any significant response to the common

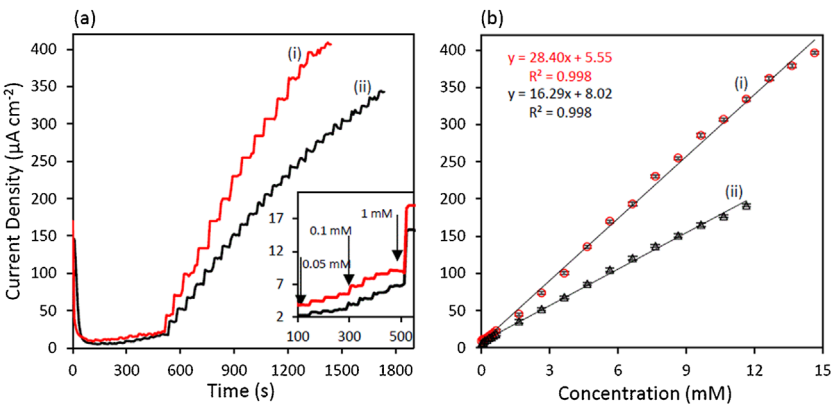

Figure 7 (a) Amperometric responses at +0.6 V with increasing glucose concentration for the electrodes (i) T_{30} (red) and (ii) S_{60} (black). (b) Electrode response as a function of glucose concentration.

Table 2 Glucose sensing by copper oxide electrodes.

electrode materials	detection potential (V)	sensitivity ($\mu A\,mM^{-1}\,cm^{-2}$)	linear range (μM)	lower detection limit (μM)	reference
nano-cubic Cu_2O/Ti (T_{30})	+0.6	28.40	17–11650	15.6	This work
microcrystalline Cu_2O/Ti (S_{60})	+0.6	16.29	30–9650	28.1	This work
octahedralCu_2O/nafion/GCE	+0.6	241	300–4100	128	[7] (2015)
Cu_2O/MWCNT	−0.20	6.53[a]	up to 10	0.05	[12] (2009)
Cu_2O/Cu	+0.60	62.29[a]	5–6750	37	[24] (2012)
graphene wrapped Cu_2O nanocubes/GCE	+0.60	285	300–3300	3.3	[26] (2013)
CQDs/octahedralCu_2O/nafion/GCE	+0.60	298	20–4300	8.4	[28] (2015)
Cu_2O nanospheres /NFs/CG	+0.50	190	5–1100	47.2	[32] (2011)
microcubes of porous Cu_2O/Nf/GCE	+0.40	10.95[a]	2–350	1.3	[33] (2010)
mesocrystalline Cu_2O hollow nanocubes modified GCE	+0.60	52.5[a]	1–1700	0.87	[34] (2012)

[a]Sensitivity is given in $\mu A\,mM^{-1}$.

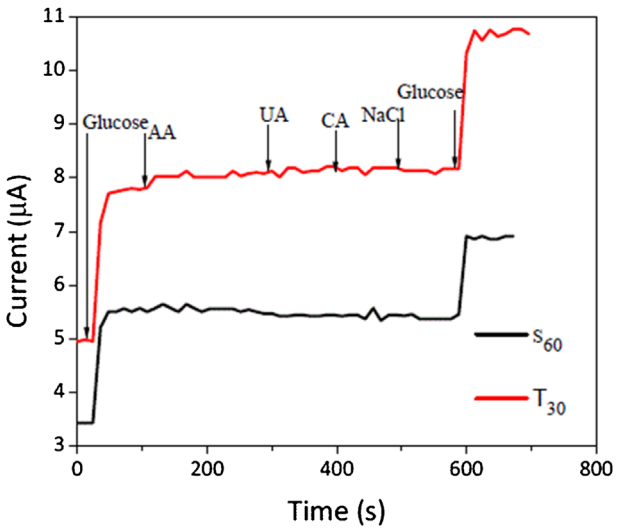

Figure 8 The interference test of the sensors of S_{60} and T_{30} in 0.1 M NaOH at +0.6 V with 0.1 mM glucose and other interferents of ascorbic acid (AA), uric acid (UA), citric acid (CA), and NACl.

interfering substances such and AA, UA, CA, and sodium chloride. In conclusion, it can be shown that the present method, which utilizes a surfactant free template-assisted electrodeposition method for fabricating nano-cubic n-Cu_2O thin films, provides a promising platform for future development of morphology-controlled non-enzymatic glucose sensors. Further enhancement in electrochemical performance could be expected by doping, surface modification, and by fabricating nano objects with definite shapes.

Acknowledgements Financial assistance from the research grant of University of Colombo, Sri Lanka (AP/3/2/2014/RG/08) is gratefully acknowledged. R. P. Wijesundara of the Department of Physics, University of Kelaniya, Sri Lanka, Dr. Nilwala Kottegoda of the Department of Chemistry and the Center for Advance Materials Research, Faculty of Applied Science at the University of Sri Jayewardenepura, Sri Lanka and K. D. R. N. Kalubowila of the Department of Physics, University of Colombo, Sri Lanka are acknowledged for the assistance provided in making some of the experimental measurements.

References

[1] K. M. D. C. Jayathilaka, V. Kapaklis, W. Siripala, and J. K. D. S. Jayanetti, Semicond. Sci. Technol. **27**, 125019 (2012).
[2] X. Zou, H. Fan, Y. Tian, M. Zhang, and X. Yan, RSC Adv. **5**, 23401 (2015).
[3] M. Pavan, S. Rühle, A. Ginsburg, D. A. Keller, Han nah-Noa Barad, P. M. Sberna, D. Nunes, R. Martins, A. Y. Anderson, A. Zaban, and E. Fortunato, Sol. Energy Mater. Sol. Cells **132**, 549–556 (2015).
[4] A. H. Jayatissa, P. Samarasekara, and G. Kun, Phys. Status Solidi A **206**, 332–337 (2009).
[5] J. L. K. Jayasinghe, K. M. D. C Jayathilaka, M. S. Gunawardene, D. P. Dissanayake, and J. K. D. S Jayanetti, Phys. Status Solidi B **254**, 1600333 (2017). https://doi.org/10.1002/pssb.201600333
[6] Y. H. Won and L. A. Stanciu, Sensors (Basel) **12**, 13019–13033 (2012).
[7] L. Wang, J. Fu, H. Hou, and Y. Song, Int. J. Electrochem. Sci. **7**, 12587–12600 (2012).
[8] X. Zou, H. Fan, Y. Tian, and S. Yan, CrystEngComm **16**, 1149 (2014).
[9] X. Zou, H. Fan, Y. Tian, M. Zhang, and X. Yan, Dalton Trans. **44**, 7811 (2015).
[10] V. Figueiredo, E. Elangovan, G. Goncalves, N. Franco, E. Alves, S. H. K. Park, R. Martins, and E. Fortunato, Phys. Status Solidi A **206**, 2143–2148 (2009).
[11] W. Siripala, K. M. D. C. Jayathilaka, and J. K. D. S. Jayanetti, J. Bionanosci. **3**, 1–6 (2009).
[12] X. Zhanga, G. Wanga, W. Zhanga, Y. Wei, and B. Fanga, Biosens. Bioelectron. **24**, 3395–3398 (2009).
[13] D. Nunes, L. Santos, P. Duarte, A. Pimentel, J. V. Pinto, P. Barquinha, P. A. Carvalho, E. Fortunato, and R. Martins, Microsc. Microanal. **21**, 108–119 (2015).
[14] C. Iida, M. Sato, M. Nakayama, and A. Sanada, Int. J. Electrochem. Sci. **6**, 4730–4736 (2011).

[15] P. E. de Jongh, D. Vanmaekelbergh, and J. J. Kelly, Chem. Mater. **11**, 3512–3517 (1999).
[16] C. Espro, N. Donato, S. Galvagno, D. Aloisio, S. G. Leonardi, and G. Neri, Chem. Eng. Trans. **41**, 415–420 (2014).
[17] Hong-Ying Yu, Miao-Qing Xu, Shu-Hong Yu, and Guang-Chao Zha, Int. J. Electrochem. Sci. **8**, 8050–8057 (2013).
[18] Liao-Chuan Jiang and Wei-De Zhang, Biosens. Bioelectron. **25**, 1402–1407 (2010).
[19] J. Luo, S. Jiang, H. Zhang, J. Jiang, and X. Liu, Anal. Chim. Acta **709**, 47–53 (2012).
[20] L. Luo, L. Zhu, and Z. Wang, Bioelechem **88**, 156–163 (2012).
[21] X. Ji, A. Wang, and Q. Zhao, J. Nanomater. (2014). Article ID 287303. https://doi.org/10.1155/2014/287303
[22] E. Reitz, W. Jia, M. Gentile, Y. Wang, and Y. Lei, Electroanalysis **22**, 2482–2486 (2008).
[23] X. Wanga, C. Hua, H. Liub, G. Dub, X. Hea, and Y. Xia, Sens. Actuators B **144**, 220–225 (2010).
[24] L. Wang, J. Fu, H. Hou, and Y. Song, Int. J. Electrochem. Sci. **7**, 12587–12600 (2012).
[25] Ai-Jun Wang, Jiu-Ju Feng, Zhong-Hua Li, Qi-Chen Liao, Zhen-Zhen Wang, and Jian-Rong Chena, CrystEngComm **14**, 1289 (2012).
[26] M. Liu, R. Liu, and W. Chen, Biosens. Bioelectron. **45**, 206–212 (2013).
[27] S. Felix, P. Kollu, B. P. C. Raghupathy, S. K. Jeong, and A. N. Grace, J. Chem. Sci. **126**, 25–32 (2014).
[28] Y. Li, Y. Zhong, Y. Zhang, W. Weng, and S. Li, Sens. Actuators B **206**, 735–743 (2015).
[29] K. M. D. C. Jayathilaka, A. M. R. Jayasinghe, G. U. Sumanasekara, V. Kapaklis, W. Siripala, and J. K. D. S. Jayanetti, Phys. Status Solidi B **252**, 1300–1305 (2015).
[30] G. Liu and Y. Lin, Electrochem. Commun. **8**, 251 (2006).
[31] H. Wei, Jian-Jun Sun, L. Guo, X. Li, and Guo-Nan Chen, Chem. Commun. **2**, 2842–2844 (2009).
[32] S. Li, Y. Zheng, G. W. Qin, Y. Ren, W. Pei, and L. Zuo, Talanta **85**, 1260–1264 (2011).
[33] L. Zhang, Y. Ni, and H. Li, Microchim. Acta **171**, 103–108 (2010).
[34] Z. Gao, J. Liu, J. Chang, D. Wu, J. He, K. Wang, F. Xu, and K. Jiang, CrystEngComm **14**, 6639–6646 (2012).